Research Statement

Shelvean Kapita

1 Research interests and background

My research interests are in Applied Mathematics, Numerical Analysis and Scientific Computing. I work on the design, analysis and implementation of numerical algorithms for solving Partial Differential Equations (PDEs) that arise in science and engineering applications. To date, I have focused on applications to wave propagation and scattering in unbounded domains and to free-boundary problems modeled by variational inequalities. Recently, I have developed algorithms for solving constrained PDEs using Bernstein-Bézier splines of arbitrary order and smoothness. I have developed specialized software in Python to implement Bernstein-Bézier spline techniques for PDEs and variational inequalities. I have also written code in MATLAB to solve frequency domain acoustic wave propagation and scattering using the Trefftz Discontinuous Galerkin Method. In the immediate future, I hope to apply Bernstein-Bézier spline methods to solve PDEs with constraints such as parabolic variational inequalities, frictional contact problems, PDE-constrained optimization, and coupled reaction-diffusion systems.

2 Current projects

The central goal of numerical PDEs is to approximate solutions of a wide class of PDEs under general conditions reliably and accurately. An ideal numerical method for solving PDEs should be able to handle complicated geometry (e.g. non-convex polygons), smooth and discontinuous coefficients, and should remain stable and accurate for a large range of discretization parameters. Standard finite element methods with low order polynomials offer geometric flexibility but have relatively low resolution. On the other hand, spectral methods, which use high polynomial degrees, offer high resolution but lack geometric flexibility. High-order *hp*-finite element methods combine the advantages of the two by offering both high resolution and geometric flexibility. However the advantages of *hp*-finite element methods are not fully realized if traditional Lagrange polynomial basis functions are utilized. The assembly of element mass and stiffness matrices using Lagrange basis functions of degree p in spatial dimension d generally require numerical integration (quadrature), and the overall computational cost of assembling an element matrix is at least $\mathcal{O}(p^{3d})$, [1] which is prohibitively expensive for large p or d.

Bernstein-Bézier polynomials on triangulations possess some key properties that make them attractive for use in high-order *hp* finite element methods. Although Bernstein-Bézier polynomials are widely used in Computer Aided Geometric Design and visualization, they are less commonly used in finite elements. Bernstein polynomials can be utilized to construct the element matrices in $\mathcal{O}(p^{2d})$ operations which is of optimal order [1].

My research seeks to apply Bernstein-Bézier finite element techniques to solve PDEs and variational inequalities. Bernstein-Bézier finite element methods combined with C^r smoothness conditions (usually in applications $r = 0, 1,$ or 2) are sometimes known as Multivariate Splines, and have been applied successfully to a range of PDEs in two and three dimensions, including the Poisson [6, 29], biharmonic [6, 30], Helmholtz [13], reaction-diffusion [16, 34], Navier-Stokes [5, 3], Maxwell eigenvalue [2], Monge-Ampére equations [4], convection-diffusion [12], among others. In a related approach, Warburton and Chan [11, 15] have developed GPU-accelerated Bernstein-Bézier algorithms within a Discontinuous Galerkin framework to solve the wave equation.

In my current work, I am extending the applications of C^r Bernstein-Bézier finite element methods to include variational inequalities, and PDE constrained optimization and optimal control problems.

2.1 Bernstein-Bézier Splines for solving elliptic variational inequalities

My current research program is focused on solving variational inequalities using high-order Bernstein-Bézier polynomials. Variational inequalities are often used to model situations with a free boundary such as frictional contact, American put options in finance, elastoplasticity, phase transformations, and questions relating to thermal expansion [28]. The free boundary is generally unknown, and its determination is part of the solution procedure. The presence of a free-boundary complicates the numerical algorithm and requires use of iterative algorithms to resolve it. In general, the solution of a variational inequality has low regularity even when the obstacle is C^∞ smooth, and as a result, a great number of papers have restricted attention to linear finite elements. However, Banz et al. [7], [8] have shown that adaptive strategies with hp-finite elements (with polynomials of degree $p = 1, 2,$ and 3) combined with mesh refinement/coursening provide an efficient method of solving variational inequalities.

A prototypical example of a variational inequality is the elliptic obstacle problem for Poisson's equation: find the displacement u of a thin elastic membrane over a region $\Omega \subset \mathbb{R}^2$ with a fixed boundary $u = g$ that is constrained to lie above a rigid obstacle ψ, and under the action of a force f.

$$\begin{cases} -\Delta u \geq f, \quad u \geq \psi \text{ in } \ \Omega, \\ (-\Delta u - f)(u - \psi) = 0 \text{ in } \Omega, \\ u = g \text{ on } \ \partial\Omega. \end{cases} \tag{1}$$

Problem (1) is equivalent to the constrained optimization problem:

$$\begin{cases} \min\limits_u J(u) = \dfrac{1}{2} \displaystyle\int_\Omega \left(|\nabla u|^2 - 2fu\right) \, dx \\ \text{s.t.} \quad u \geq \psi \text{ in } \ \Omega, \quad u = g \text{ on } \ \partial\Omega. \end{cases} \tag{2}$$

where the minimization is taken over $H^1(\Omega)$ functions that satisfy the given constraints. This reformulation (2) is crucial to our derivation of the numerical algorithm.

The first inequality in (1) is eliminated by introducing a non-negative Lagrange multiplier λ defined as the element residual $\lambda := -\Delta u - f$. The problem is now to determine the pair (u, λ) such that:

$$\begin{cases} -\Delta u - \lambda = f, \quad u \geq \psi \text{ in } \Omega, \\ \lambda \geq 0, \quad \lambda(u - \psi) = 0 \text{ in } \Omega, \\ u = g \text{ on } \partial\Omega. \end{cases} \tag{3}$$

In [23], I use Bernstein-Bézier polynomials of arbitrary degree as shape functions to discretize the system (3). Numerical experiments show that globally continuous quadratics and cubics, combined with residual based adaptive mesh refinement, are generally more efficient than linear elements. In practice, however, polynomials of degree $p \geq 4$ do not offer significant advantages for the obstacle problem due to the low regularity of the solutions $u \notin H^3$.

To give some details of the discretization of (3), the global solution space $V_h \subset L^2(\Omega_h)$ over a triangular mesh Ω_h consists of elementwise discontinuous Bernstein-Bézier polynomials $\{\varphi_j\}$ of degree not greater than $p \in \mathbb{N}$ where each triangle supports $\binom{p+2}{2}$ basis functions. The discrete solution is then to find a pair $(u_h, \lambda_h) \in V_h \times V_h^+$ such that $V_h = \text{span}\{\varphi_1, \cdots, \varphi_N\}$ where $N = n_t\binom{p+2}{2}$ is the total number of basis functions on the triangulation, with n_t the number of triangles in the mesh, and $V_h^+ \subset V_h$ consists of piecewise polynomials of degree p with non-negative coefficients.

$$\begin{cases} (\nabla_h u_h, \nabla_h v_h) - (\lambda_h, v_h) = (f_h, v_h), \quad \forall v_h \in V_h \\ (u_h - \psi_h, \mu_h) \geq 0, \quad \forall \mu_h \in V_h^+ \\ (u_h - \psi, \lambda_h) = 0, \\ u_h = g_h \text{ on } \partial\Omega_h. \end{cases} \tag{4}$$

with $(\cdot,\cdot)$ representing the $L^2(\Omega_h)$ norm, and ∇_h the element-wise gradient.

In matrix form, (4) can be written as:

$$\begin{cases} A\mathbf{c} - \boldsymbol{\sigma} = \mathbf{f} \\ \boldsymbol{\sigma} \geq 0, \quad M\mathbf{c} - \boldsymbol{\psi} \geq 0, \quad \boldsymbol{\sigma}^T(M\mathbf{c} - \boldsymbol{\psi}) = 0, \\ B\mathbf{c} = \mathbf{g}. \end{cases} \tag{5}$$

where A, M are the stiffness and mass matrices with components

$$A_{ij} = (\nabla\varphi_j, \nabla\varphi_i), \quad M_{ij} = (\varphi_j, \varphi_i), \quad i, j = 1, \cdots, N$$

respectively, $\mathbf{f}_j = (f, \varphi_j)$, $\boldsymbol{\psi}_j = (\psi, \varphi_j)$ are the components of the load vector and obstacle moments respectively. The vector $\mathbf{c}$ comprises of the coefficients of u_h with respect to the basis $\{\varphi_j\}$, $\boldsymbol{\sigma}_j = (\lambda_h, \varphi_j)$, and $B\mathbf{c} = \mathbf{g}$ is the discretization of the boundary condition.

The discrete Lagrange multipliers $\boldsymbol{\lambda}$ are recovered from $\boldsymbol{\sigma} := M\boldsymbol{\lambda}$ by an inversion of the mass matrix M. In practice, we do not invert the mass matrix, but replace it by an approximate diagonal lumped-mass matrix, $\overline{M}$. The diagonal lumped-mass matrix is particularly simple to compute in the Bernstein-Bezier basis in 2D:

$$\overline{M}_{jj} = \frac{2A_j}{(p+1)(p+2)},$$

where A_j is the area of the triangle at degree of freedom j. The entries of $\bar{M}$ are positive for a non-degenerate mesh. Inversion of $\bar{M}$ amounts to taking the reciprocals of the diagonal entries of $\overline{M}$.

The *complementarity conditions* in the second line of (4) can be written equivalently as an equality, as shown in [17],

$$\boldsymbol{\sigma} - \max\{0, \boldsymbol{\sigma} + \alpha(M\mathbf{c} - \boldsymbol{\psi})\} = 0.$$

It is known (e.g. Rodrigues [33] for instance) that for the elliptic obstacle problem (1) if the domain is convex or the boundary is $C^{1,1}$ smooth, and the data is such that $f \in L^2(\Omega)$ with $\psi \in H^2(\Omega)$, $g \in H^{3/2}(\partial\Omega)$, $\psi \leq g$ on $\partial\Omega$, then $u \in H^2(\Omega)$ and $\lambda \in L^2(\Omega)$. The key idea of the Bernstein-Bézier spline method is that although V_h is discontinuous, *smoothness of u_h is imposed via a system of linear constraints* called the smoothness conditions (see Awanou et al. [6]). In matrix form, the smoothness conditions take the form $S\mathbf{c} = 0$, where the matrix S depends only on the polynomial degree p, smoothness r (i.e. $u_h \in C^r$), and the mesh. For Bernstein-Bézier polynomials, the smoothness matrix S is assembled easily during pre-computation. Although the degree of smoothness $r \geq 0$ can be chosen arbitrarily in the construction of S, numerical results [23] show that $r = 0$ is the most stable for the elliptic obstacle problem (4) using our scheme. This is due to the low regularity of solutions of obstacle problems. For general problems, C^1 or C^2 solutions can be computed easily in this framework simply by changing the parameter $r \geq 0$.

Finally, adding the smoothness constraints for u_h, the problem is reduced to solving for $(\mathbf{c}, \boldsymbol{\lambda}, \boldsymbol{\mu})$ that satisfies $\boldsymbol{\sigma} = \overline{M}\boldsymbol{\lambda}$ and

$$\begin{cases} A\mathbf{c} - \boldsymbol{\sigma} + \boldsymbol{\mu}^T(Q\mathbf{c} - \mathbf{G}) = \mathbf{f}, \quad Q\mathbf{c} = \mathbf{G}, \\ \boldsymbol{\sigma} - \max\{0, \boldsymbol{\sigma} + \alpha(M\mathbf{c} - \boldsymbol{\psi})\} = 0, \quad \alpha > 0. \end{cases} \tag{6}$$

where $\overline{M}$ is the diagonal lumped-mass matrix, $Q = [S; B]$ and $\mathbf{G} = [0; \mathbf{g}]$ are the combined equality constraint matrices and right hand sides, and $\boldsymbol{\mu}$ is the vector of Lagrange multipliers enforcing the smoothness and boundary conditions.

2.2 Optimization techniques for solving singular Quadratic Programs with equality and inequality constraints

The main challenge in solving (6) is that the stiffness matrix A is only positive-semidefinite and singular. It turns out that (6) is the Karush Kuhn Tucker (KKT) optimality condition for a constrained quadratic minimization problem with equality and inequality constraints. That is

$$\begin{cases} \min\limits_{\mathbf{c} \in \mathbb{R}^N} J_h(\mathbf{c}) := \dfrac{1}{2}\mathbf{c}^T A\mathbf{c} - \mathbf{c}^T\mathbf{f}, \\ \text{s.t.} \quad M\mathbf{c} \geq \boldsymbol{\psi}, \quad Q\mathbf{c} = \mathbf{G}. \end{cases} \tag{7}$$

which is a discretization of the constrained minimization problem (2). In our case, the matrix A is positive-definite when restricted to the kernel of the constraint matrix $Q = [S; B]$ formed by concatenating the smoothness and boundary matrices. Hence, the augmented matrix $A_\varrho := A + \varrho Q^T Q$ is invertible for $\varrho > 0$. The non-linear system of equations (6) is solved using the Primal Dual Active Set method (PDAS), with the matrix A replaced by the augmented matrix A_ϱ.

Our PDAS iterative algorithm consists of two loops. In the outer loop, an approximate active set is identified, and in the inner loop a linear system is solved inexactly by the Uzawa algorithm to identify the solution in the inactive set. We choose one step only in the Uzawa solver for each iteration. This avoids needless computations before the active set has been identified. However once the active set has been identified, the Uzawa algorithm converges exponentially per step towards the discrete solution as shown in Figures 1, 2.

In the next step, the solution $\mathbf{c}$ and Lagrange multipliers $\boldsymbol{\lambda}$ are used to derive residual error estimators derived in [8] to drive the mesh refinement.

At first glance, solving (6) to approximate the solution of the obstacle problem (1) looks inefficient, since at each iteration, we solve for a triple $(\mathbf{c}_n, \boldsymbol{\lambda}_n, \boldsymbol{\mu}_n)$ when we need $\mathbf{c}_n$ only. However, each PDAS iteration updates multiple active indices at once, followed by one iteration of the Uzawa algorithm involving a sub-matrix of A_ϱ at the inactive indices. The Lagrange multipliers $\boldsymbol{\lambda}_n$ and $\boldsymbol{\mu}_n$ are updated using the solution $\mathbf{c}_n$ and matrix multiplications. This way of solving the problem is more efficient than a direct solution that solves for the triple at once.

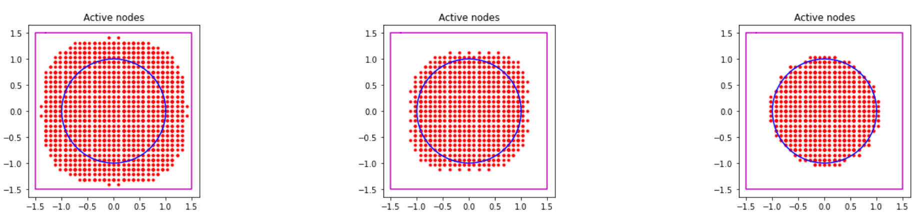

(a) initial (b) 5 iterations (c) 10 iterations

Figure 1: Distribution of active nodes during the iterative solution of (6). In this example, the discrete coincidence set is identified after about 10 iterations. The blue circle represents the true free boundary. Here $p = 3$ and the exact solution is given in (8).

2.3 Numerical Results for the Elliptic Obstacle Problem

In order to test the convergence of the Bernstein-Bézier scheme (6) for the elliptic obstacle problem (1), we choose a known exact solution. Results are shown in Fig 3.

Let $\Omega = (-1.5, 1.5)^2, f = -2, \psi = 0$ and $g = r^2/2 - \ln(r) - 1/2$ be the boundary data on $\partial\Omega$, where $r^2 = x^2 + y^2$. The exact solution is given by

$$u = \begin{cases} r^2/2 - \ln(r) - 1/2, & \text{if } r \geq 1 \\ 0 & \text{otherwise} \end{cases} \tag{8}$$

2.4 Implementation in Python

I have implemented the algorithm for solving the elliptic obstacle problem in Python. The project is composed of four main modules: 2D meshes and geometry, constructions and

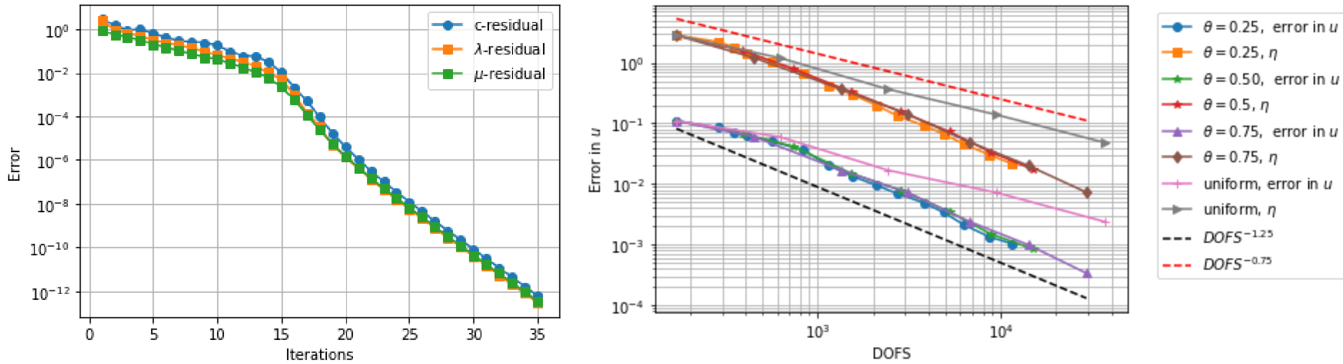

(a) Residuals vs iterations

(b) $p = 3$

Figure 2: (a) Typical convergence graph of residuals $\|\mathbf{c}_{n+1} - \mathbf{c}_n\|_\infty$, $\|\boldsymbol{\lambda}_{n+1} - \boldsymbol{\lambda}_n\|_\infty$ and $\|\boldsymbol{\mu}_{n+1} - \boldsymbol{\mu}_n\|_\infty$ vs number of iterations. Asymptotic convergence coincides with identification of the active set. Here $p = 3$ on an adaptively refined mesh. (b) convergence of $\|\nabla(u - u_h)\|$ and error estimator η for refinement parameters $\theta = 0.25, 0.5, 0.75,$ and 1. Adaptively refined meshes are more efficient for the obstacle problem than uniformly refined meshes.

algorithms for Bernstein-Bézier polynomials, algorithms for assembly of matrices, and non-linear solvers. Some of the modules are translations to Python of an earlier MATLAB code for the Poisson equation written mostly by Ming-Jun Lai at the University of Georgia. However, I have made several improvements to this earlier code.

- The coefficient vectors $\mathbf{c}$, $\boldsymbol{\lambda}$ are used to evaluate the discrete solutions u_h and λ_h using tensor algorithms proposed by Ainsworth et al. in [1]. Compared with a previous version that used the de-Casteljau algorithm, the new evaluation algorithm is fast. For example to evaluate a solution vector of length 688,128 on a mesh with 33,768 triangles at about 13 million points took only 1.4 seconds on an 8GB RAM laptop. Using the previous algorithm, this computation took several minutes. I am working on speeding up these algorithms further using parallel Python `mpi4py` and GPUs.

- The (local) mass and stiffness matrices are assembled using the optimal algorithms presented by Ainsworth et al. in [1].

- I assemble the (global) mass and stiffness matrices directly as 3D tensors, rather than looping through the mesh elements. The third dimension being the triangle enumeration. In this case, sparse linear algebra is not needed but tensor algebra using the Python package `numpy`. Matrix-matrix and matrix-vector multiplications become tensor dot products and contractions which are computed by `numpy.tensordot`. For large p and number of triangles, assembly time can be reduced by using 3D tensor algebra in `numpy`.

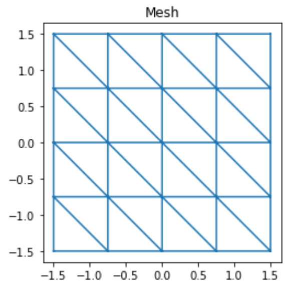

(a) initial mesh

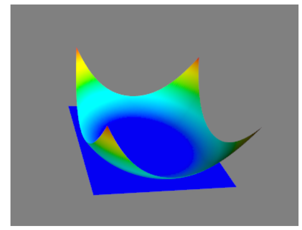

(b) solution and obstacle

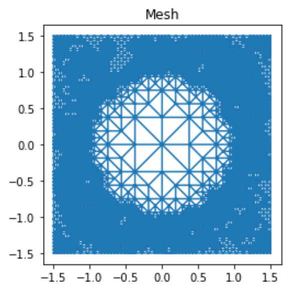

(c) $p = 1$ adaptive mesh

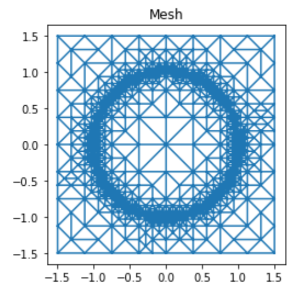

(d) $p = 3$ adaptive mesh

Figure 3: Solution of the obstacle problem using Bernstein-Bézier polynomials. Adaptive meshes after 10 cycles for polynomial degrees $p = 1$ and 3 using residual based error estimators. When $p = 1$, the algorithm refines the mesh where the solution is nonlinear, i.e. outside the contact zone. For $p = 3$, the algorithm mostly refines the region around the free-boundary.

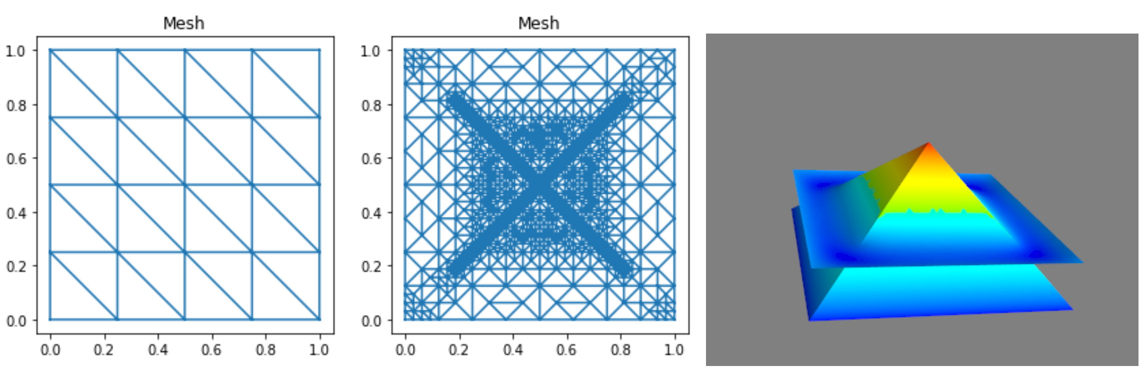

(a) initial mesh (b) mesh after 14 cycles (c) solution and obstacle

Figure 4: Solution of the obstacle problem with a pyramid obstacle using $p = 2$ polynomials with C^0 continuity. The adaptive algorithm refines along the sharp edges of the pyramid obstacle.

3 Extensions

Immediate extensions of my work on Bernstein-Bézier methods for the 2D elliptic obstacle problem are:

- extension to the 3D obstacle problem where efficiency gains made in 2D will be of crucial importance.
- parabolic obstacle problems, including applications to American options from finance
- PDE constrained optimal control problems fit naturally into our solution process. In this case, however, the constraint matrices are derived from discretizing the PDE. Therefore, we expect that most of our code will be reused to solve PDE constrained optimal control problems.
- the Signorini problem is a direct variant of the elliptic obstacle problem. The only difference is that for the Signorini problem, the obstacle is restricted to the boundary of the domain.
- application to three dimensional frictional contact problems in mechanics.
- systems of reaction-diffusion equations have been applied to some problems in biological sciences and chemistry including pattern formation. A high-order treatment using Bernstein-Bézier polynomials may be useful for applications of reaction-diffusion equations to pattern formation which require high resolution.

4 Time-harmonic wave scattering

I have worked on numerical methods for solving time-harmonic wave scattering problems in unbounded domains. Most of the challenges in numerical wave propagation arise from the following situations:

(a) resolving high wavenumber solutions efficiently and inexpensively.

(b) devising transparent boundary conditions to solve unbounded domain wave equations in a finite computational region.

(c) devising numerical methods to model wave propagation through inhomogeneous or structured media.

(d) devising methods for mesh refinement to improve efficiency of numerical methods.

My work to address these questions is published in [24, 25, 27, 26].

4.1 Trefftz Discontinuous Galerkin Methods for solving time-harmonic wave equations with transparent boundary conditions

The Trefftz method, in which simple local solutions of a PDE are used as basis functions in the finite element approximation of the global solution, was conceived by Erich Trefftz in the 1920s. The main idea of the Trefftz method is that one can use integration by parts to eliminate all internal volume degrees of freedom and remain with an equivalent problem that is posed on the edges of the mesh.

The idea of the Trefftz method was reconceived and developed by Cessenat and Després for the Helmholtz equation under the name Ultra Weak Variational Formulation (UWVF) [9, 10]. The UWVF was shown by Hiptmair et al. [14, 18, 19, 20] to be a special case of the discontinuous Galerkin method with plane wave basis functions (PWDG). The UWVF and PWDG have been extended to include wave equations such as the Maxwell equations [35, 22], elastic waves [32, 31], and fluid-solid interaction [21].

Most wave propagation problems in applications are posed in unbounded domains. Therefore one needs to truncate the unbounded domain to a finite domain in order to find a numerical solution. A naïve discretization using standard boundary conditions would lead to inaccurate results, one needs transparent boundary conditions to prevent waves from reflecting off the boundary. As a first approximation, standard Robin boundary conditions have been used in PWDG methods. I devised a method to incorporate accurate Dirichlet-to-Neumann boundary conditions into the PWDG method to improve their accuracy in modeling unbounded wave phenomena. Results of this work are published in [24, 25, 26].

References

[1] M. Ainsworth, G. Andriamaro, and O. Davydov. Bernstein-Bézier finite elements of arbitrary order and optimal assembly procedures. *SIAM Journal on Scientific Computing*, 33:3087–3109, 2011.

[2] M. Ainsworth, G. Andriamaro, and O. Davydov. A Bernstein-Bézier Basis for Arbitrary Order Raviart-Thomas Finite Elements. *Constructive Approximation*, 41(1):1–22, Feb 2015.

[3] G. Awanou. *Energy methods in 3D spline approximations of the Navier-Stokes equations*. PhD thesis, University of Georgia, 2003.

[4] G. Awanou. Spline element method for Monge-Ampère equations. *BIT Numerical Mathematics*, 55(3):625–646, 2015.

[5] G. Awanou and M.-J. Lai. Trivariate spline approximations of 3D Navier-Stokes equations. *Mathematics of Computation*, 74(250):585–601, 2005.

[6] G. Awanou, M.-J. Lai, and P. Wenston. The Multivariate Spline Method for Scattered Data Fitting and Numerical Solutions of Partial Differential Equations. In G. Chen and M.-J. Lai, editors, *Wavelets and Splines*, pages 24–74. Nashboro Press, Nashville, TN, 2006.

[7] L. Banz, B.P. Lamishhane, and E.P. Stephan. Higher-order FEM for the obstacle problem of the p-Laplacian-A variational inequality approach. *Computers and Mathematics with Applications*, 2017.

[8] L. Banz and E. Stephan. A posteriori error esrimates of *hp*-adaptive IPDG-FEM for elliptic obstacle problems. *Applied Numerical Mathematics*, 76:76–92, 2014.

[9] O. Cessenat and B. Després. Application of an Ultra Weak Variational Formulation of elliptic PDEs to the two-dimensional Helmholtz problem. *SIAM journal on numerical analysis*, 35(1):255–299, 1998.

[10] O. Cessenat and B. Després. Using plane waves as base functions for solving time harmonic equations with the Ultra Weak Variational Formulation. *Journal of Computational Acoustics*, 11(02):227–238, 2003.

[11] J. Chan and Warburton T. GPU-Accelerated Bernstein-Bézier Discontinuous Galerkin Methods for Wave Problems. *SIAM J. Sci. Comput.*, 39, 2017.

[12] M. El-Amrani, A. El-Kacimi, B. Khouya, and M. Seaid. Bernstein-Bézier Galerkin-Characteristics Finite Element Method for Convection-Diffusion problems. *Journal of Scientific Computing*, 92(2):1–29, 2022.

[13] A. El-Kacimi, O. Laghrouche, M.S. Mohamed, and J. Trevelyan. Bernstein–bézier based finite elements for efficient solution of short wave problems. *Computer Methods in Applied Mechanics and Engineering*, 343:166–185, 2019.

[14] C.J. Gittelson, R. Hiptmair, and I. Perugia. Plane Wave Discontinuous Galerkin methods: analysis of the h-version. *ESAIM: Mathematical Modelling and Numerical Analysis*, 43(2):297–331, 2009.

[15] K. Guo and J. Chan. Bernstein-Bézier weight-adjusted discontinuous Galerkin methods for wave propagation in heterogeneous media. *Journal of Computational Physics*, 400:108971, 2020.

[16] J.B. Gutierrez, M.-J. Lai, and G. Slavov. Bivariate spline solution of time dependent nonlinear PDE for a population density over irregular domains. *Mathematical Biosciences*, 270:263–277, 2015.

[17] M. Hintermüller, K. Ito, and K. Kunisch. The primal-dual active set strategy as a semismooth Newton method. *SIAM Journal on Optimization*, 13(3):865–888, 2003.

[18] R. Hiptmair, A. Moiola, and I. Perugia. Plane Wave Discontinuous Galerkin Methods for the 2D Helmholtz equation: analysis of the p-version. *SIAM Journal on Numerical Analysis*, 49(1):264–284, 2011.

[19] R. Hiptmair, A. Moiola, and I. Perugia. Error analysis of Trefftz-discontinuous Galerkin methods for the time-harmonic Maxwell equations. *Mathematics of Computation*, 82(281):247–268, 2013.

[20] R. Hiptmair, A. Moiola, and I. Perugia. A survey of trefftz methods for the helmholtz equation. In *Building bridges: connections and challenges in modern approaches to numerical partial differential equations*, pages 237–279. Springer, 2016.

[21] T Huttunen, JP Kaipio, and P Monk. An ultra-weak method for acoustic fluid–solid interaction. *Journal of Computational and Applied Mathematics*, 213(1):166–185, 2008.

[22] Tomi Huttunen, Matti Malinen, and Peter Monk. Solving Maxwell's equations using the Ultra Weak Variational Formulation. *Journal of Computational Physics*, 223(2):731–758, 2007.

[23] S. Kapita. A Bernstein-Bézier finite element method for solving the Elliptic Obstacle problem. *under preparation.*

[24] S. Kapita. *Plane Wave Discontinuous Galerkin Methods for Acoustic Scattering*. PhD thesis, University of Delaware, 2016.

[25] S. Kapita and P. Monk. A Plane Wave Discontinuous Galerkin Method with a Dirichlet-to-Neumann boundary condition for the scattering problem in acoustics. *Journal of Computational and Applied Mathematics*, 327:208–225, 2018.

[26] S. Kapita, P. Monk, and V. Selgas. A Trefftz Discontinuous Galerkin method for time-harmonic waves with a generalized impedance boundary condition. *Applicable Analysis*, 99(3):379–406, 2020.

[27] S. Kapita, P. Monk, and T. Warburton. Residual-based adaptivity and PWDG methods for the Helmholtz equation. *SIAM Journal on Scientific Computing*, 37(3):A1525–A1553, 2015.

[28] D. Kinderlehrer and G. Stampacchia. *An Introduction to Variational Inequalities and Their Applications*, volume 31 of *Classics in Applied Mathematics*. SIAM, 1987.

[29] M-J. Lai and J. Lee. A Multivariate Spline Based Collocation Method for Numerical Solution of Partial Differential Equations. *SIAM Journal on Numerical Analysis*, 60(5):2405–2434, 2022.

[30] M.-J. Lai, C. Liu, and P. Wenston. Numerical simulations on two nonlinear biharmonic evolution equations. *Applicable Analysis*, 83(6):563–577, 2004.

[31] T. Luostari, T. Huttunen, and P. Monk. Error estimates for the ultra weak variational formulation in linear elasticity. *ESAIM: Mathematical Modelling and Numerical Analysis*, 47(1):183–211, 2013.

[32] Andrea Moiola. Plane wave approximation in linear elasticity. *Applicable Analysis*, 92(6):1299–1307, 2013.

[33] J.F. Rodrigues. *Obstacle Problems in Mathematical Physics*, volume 134 of *North-Holland Mathematical Studies*. North Holland, 1987.

[34] G. Slavov. *Bivariate spline solution to a class of reaction-diffusion equations*. PhD thesis, University of Georgia, 2016.

[35] Long Yuan, Qiya Hu, et al. Error analysis of the Plane Wave Discontinuous Galerkin method for Maxwell's equations in anisotropic media. *Commun. Comput. Phys.*, 25:1496–1522, 2019.